ESR study of the anisotropic exchange in the quasi-one-dimensional antiferromagnet $Sr_2V_3O_9$

V. A. Ivanshin,[1,2] V. Yushankhai,[1,3] J. Sichelschmidt,[1] D. V. Zakharov,[2] E. E. Kaul,[1] and C. Geibel[1]
[1]*Max-Planck-Institut für Chemische Physik fester Stoffe, D-01187 Dresden, Germany*
[2]*MRS Laboratory, Kazan State University, 420008 Kazan, Russia*
[3]*Joint Institute for Nuclear Research, 141980 Dubna, Russia*
(Received 21 March 2003; published 5 August 2003)

The chainlike spin-1/2 antiferromagnetic vanadium oxide compound $Sr_2V_3O_9$ is studied by electron spin resonance (ESR) with special attention to the space distribution of the Dzyaloshinskii-Moriya (DM) vector along magnetic chains. The angular variation and the temperature dependence of the ESR linewidth is measured in two different planes of a single crystal in the temperature range 4.2–500 K. The ESR data interpretation is based on the combined application of the standard ESR theory for low-dimensional systems and an updated theory using a hidden symmetry in the antiferromagnetic spin-1/2 chain model with the staggered DM interaction. As a result, a DM interaction with a more general (nonstaggered) spatial distribution of DM vectors is claimed to be responsible for the magnetic properties of the chainlike system $Sr_2V_3O_9$.

DOI: 10.1103/PhysRevB.68.064404 PACS number(s): 75.50.Ee, 75.30.Et, 76.30.−v

I. INTRODUCTION

Vanadium oxides display complex structural, electric, and magnetic properties due to the ability of vanadium to adopt several oxidation states and oxygen environment. The arrangement of VO_n $(n=4,5,6)$ polyhedra is extremely diverse and results in numerous original structures.[1] The vanadium oxides forming chain structures are of particular importance since they are expected to give new spin systems with pronounced quasi-one-dimensional (quasi-1D) magnetic properties.

Recently a quasi-1D magnetic behavior was clearly revealed in the chainlike compound $Sr_2V_3O_9$ by means of magnetic susceptibility $\chi(T)$ and the specific heat $C_p(T)$ measurements in polycrystalline samples.[2] The data are compatible with spin $S=1/2$ antiferromagnetic (AFM) Heisenberg chain model with nearest-neighbor exchange $J\simeq 82$ K and much weaker interchain coupling that leads to three-dimensional AFM ordering at the Néel temperature $T_N \simeq 5$ K. In addition, an anomalous Curie-like upturn of $\chi(T)$ was found at $T>T_N$ and claimed to be of intrinsic nature because the effect of paramagnetic impurities was ruled out by the analysis of experimental data. By analogy with Cu-compounds,[3–5] in Ref. 2 the intrachain staggered Dzyaloshinskii-Moriya (DM) interaction is proposed to be responsible for the anomalous low-T behavior of $\chi(T)$ in $Sr_2V_3O_9$. Actually, as explained in Ref. 2, the alternating tilt of the VO_6 octahedra that form the magnetic chains in $Sr_2V_3O_9$ suggests a staggered character of the DM vector and of the g-tensor distribution along magnetic chains.

The theory of a staggered magnetic susceptibility induced by a uniform magnetic field applied to the AFM spin-1/2 chain with alternating DM interaction or/and alternating g-tensor is well elaborated.[5] The theory was successfully applied[3] to pyrimidine Cu dinitrate, which is regarded as an almost ideal AFM chain system. Considering $Sr_2V_3O_9$, however, the existing theory of the low-T staggered magnetic susceptibility has to be extended to take into account weak interchain exchange coupling. Moreover, the parameters of the intrachain exchange anisotropy in $Sr_2V_3O_9$ are not yet determined. Anisotropic spin-spin interactions have to be measured and explained in close connection with structural peculiarities of $Sr_2V_3O_9$. The ESR method is a powerful tool to solve this problem.

In the present paper we report and discuss ESR data obtained on a single crystal of $Sr_2V_3O_9$ in a wide range of temperature, 4.2 K$<T<$500 K. As the main purpose of the paper, we show that the single-crystal ESR data obtained from measurements in the paramagnetic high-T limit allow us to evaluate the parameters of the dominant anisotropic interaction in the chainlike compound $Sr_2V_3O_9$.

Recently a new theoretical approach to the ESR study of quantum spin chain systems was developed.[6,7] The approach is based on an equivalent description of spin variables by applying a properly defined nonuniform unitary transformation (rotation) in spin space. When interpreting ESR data in $Sr_2V_3O_9$ we use and develop further basic ideas of this approach. Since in $Sr_2V_3O_9$ the staggered component $g^{(s)}$ of the alternating g tensor is rather small (Sec. IV), a dominant anisotropy of the *intrachain* spin interaction is expected to provide the main source for the observed ESR linewidth broadening. Therefore, we rely our analysis on the AFM spin-1/2 chain Hamiltonian

$$H=\sum_{\ell}\{J\mathbf{S}_{\ell}\mathbf{S}_{\ell+1}+\mathbf{D}_{\ell,\ell+1}(\mathbf{S}_{\ell}\times\mathbf{S}_{\ell+1})+\mathbf{S}_{\ell}\cdot\mathbf{\Gamma}_{\ell,\ell+1}\cdot\mathbf{S}_{\ell+1}\}, \tag{1.1}$$

where the antisymmetric DM interaction term $\sim\mathbf{D}_{\ell,\ell+1}$ and the symmetric exchange anisotropy $\sim\Gamma^{\alpha\beta}_{\ell,\ell+1}$ $(\alpha,\beta=x,y,z)$ are involved. In particular, below we argue that in the chain system (1.1) with a *staggered* DM interaction a residual symmetric exchange anisotropy that dominates the ESR linewidth broadening in the high-T regime is much weaker than that predicted in Ref. 7. Consequently, we show that the AFM chain model with the staggered DM vector distribution is incomplete to describe the properties of $Sr_2V_3O_9$ and a more general model of DM anisotropy has to be involved to reach a consistent description of the ESR data observed in this chainlike compound.

The outline of the paper is as follows. In Sec. II, we develop a theoretical analysis, which allows us to establish

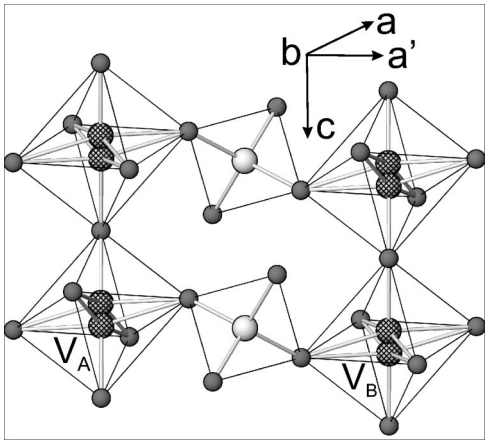

FIG. 1. Cutout of the VO layer of $Sr_2V_3O_9$. The *b* axis points perpendicular to the paper plane. The big checked circles are V^{4+}, the small dark gray ones are oxygen, and the light gray ones are V^{5+}. Corner sharing VO_6 octahedra form chains along the *c*-axis. The octahedra are shown with two feasible positions of the magnetic V^{4+} ions. Within each chain the magnetic V^{4+} ions are displaced equally from the octahedron centers. The structure with the in-phase (antiphase) orientation of the V-ion displacements of two neighboring chains is referred to as the $F(AF)$ configuration. VO^4 tetrahedra contain nonmagnetic V^{5+} ions and mediate the dominant superexchange interaction between each AB pair of the neighboring V^{4+} ions. Thus, the magnetic chains are running approximately along the a'-axis.

the relation between lattice properties of $Sr_2V_3O_9$ and the distribution of DM vector along magnetic chains. An estimate for the strongly reduced ESR linewidth expected in the spin chain system (1.1) with the staggered DM interaction is given there as well. In Sec. III, some experimental details are discussed shortly. The experimental results of the ESR measurements and their interpretation are presented in Sec. IV. The summary and concluding remarks can be found in Sec. V.

II. CRYSTAL STRUCTURE AND PRELIMINARY ANALYSIS OF THE EXCHANGE ANISOTROPY IN $Sr_2V_3O_9$

In monoclinic $Sr_2V_3O_9$ the structural chains run along the crystallographic *c* axis and are formed by corner-sharing VO_6 octahedra (Fig. 1). Neighboring structural chains are connected by VO_4 tetrahedra forming VO-layer lying in the *ac* plane, while adjacent VO layers are separated along *b* direction by Sr layers. VO_6 octahedra contain magnetic V^{4+} ions (d^1 state), while the VO_4 tetrahedra with nonmagnetic V^{5+} ions (d^0 state) serve as bridging complexes mediating superexchange (SE) between spin-1/2 octahedral V ions. It was argued[2] that the largest SE interaction with the isotropic exchange constant $J \simeq 82$ K is not *along* the structural chains but *perpendicular* to them. More precisely, a magnetic chain can be viewed as a sequence of VO_6 octahedra joined through nonmagnetic VO_4 complexes running approximately along the auxiliary axis $\mathbf{a}' \| (\mathbf{b} \times \mathbf{c})$, where **b** and **c** are orthogonal crystallographic axes in monoclinic $Sr_2V_3O_9$ (see Fig. 1). The magnetic chains are coupled along the *c* direction with the exchange constant $J_\perp$ ($10^{-2} < J_\perp/J < 10^{-1}$), and the coupling J' along the *b* direction is much weaker, $J' \ll J_\perp$.[2]

If one is interested in the anisotropy of the spin interaction in $Sr_2V_3O_9$, two structural features deserve special attention, namely, an alternating tilt of VO_6 octahedra forming a magnetic chain and a 2D spatial pattern of the off-center displacement of magnetic V-ions in the VO_6 octahedra. In close relation to the discussion in Ref. 2, we distinguish for a particular layer two possible ground-state configurations of the V ion off-center static displacements, which we refer below for brevity to as intralayer *F* and *AF* configurations. In the intralayer *F*/*AF* configuration the orientation of the V-ion off-center displacements of two neighboring structural chains are in phase/antiphase as explained also in Fig. 1. It is not clear yet[2] which of these two configurations dominates the real ground-state structure of $Sr_2V_3O_9$. In the remaining part of this section, we develop a theoretical analysis to predict the DM vector distribution along a magnetic chain for both hypothetical space patterns of the off-center V-ion displacements. The analysis shows rather different distributions of DM vectors in structural *F* and *AF* configurations. These distributions can be measured by ESR.

For each V ion shifted from the octahedral center the low-symmetry environment splits *d* orbitals to give a nondegenerate singly occupied ground-state orbital $|0\rangle$ at the energy E_0 and excited $|m\rangle$ orbitals at higher energies E_m ($m = 1, \ldots, 4$). We assume the limit of a weak spin-orbit coupling, $(E_m - E_0) = \Delta_m \gg \lambda$, since for V^{4+} ion the spin-orbit coupling constant λ is rather small, $\lambda \simeq 0.03$ eV.[8] This limit is also compatible with a weak deviation of the *g* factor from the free electron value, which is measured in $Sr_2V_3O_9$ by ESR (Sec. IV). Note also that a quantitative description of the V^{4+} ion *d*-orbital splitting in a closely related compound $Ba_2V_3O_9$ is given in Ref. 9.

For a pair V_A-V_B of neighboring V ions in a magnetic chain, we define effective transfer integrals $t_{Am,Bm'}$, describing an electron hopping between the $|m'_B\rangle$ orbital of V_B-ion and the $|m_A\rangle$ orbital of V_A ion. These transfer integrals are real and obey the relation $t_{Am,Bm'} = t_{Bm',Am}$. In this notation, the exchange constant $J = J_{AB}$ of an (AB) pair in the ground-state orbital configuration is given by the familiar expression $J_{AB} = 4t^2_{A0,B0}/U$, where *U* is the on-site Coulomb repulsion (Hubbard energy) for the *d* shell of V ion. The spin-orbit coupling mixes *d*-orbital states on each V ion and thus produces intermediate *singly* excited electron configurations of a V_A-V_B pair. Within the standard SE theory, the exchange couplings $J_{B0,Am}$ and $J_{A0,Bm}$ between the ground state and different singly excited intermediate configurations are estimated as $J_{B0,Am} = 2t_{A0,B0}t_{B0,Am}/U$ and $J_{A0,Bm} = 2t_{A0,B0}t_{A0,Bm}/U$. The lowest-order expression for the DM vector $\mathbf{D}_{AB}$ can now be written as[10,11]

$$\mathbf{D}_{AB} = -2i \sum_{m \neq 0} \left[\frac{\lambda}{\Delta^A_m} \langle m_A | \mathbf{L}_A | 0_A \rangle J_{B0,Am} - \frac{\lambda}{\Delta^B_m} \langle m_B | \mathbf{L}_B | 0_B \rangle J_{A0,Bm} \right]. \quad (2.1)$$

Here $\langle m_{A/B}|\mathbf{L}_{A/B}|0_{A/B}\rangle$ denotes matrix element of the orbital angular momentum operator. In the further discussion, we adopt local coordinate systems attached to $[VO_6]_A$ and $[VO_6]_B$ octahedra when calculating matrix elements of $\mathbf{L}_A$ and $\mathbf{L}_B$, respectively. To connect the properties of the DM vector with the structural peculiarities of $Sr_2V_3O_9$, it is convenient to rearrange slightly expression (2.1) in the following way. In general, by noting that $t_{B0,Am} \neq t_{A0,Bm}$, we introduce the quantity $I_{AB}^{(m)} = t_{A0,B0}(t_{A0,Bm} - t_{B0,Am})/U$ as a measure of the SE path asymmetry in the mth channel together with the average $J_{AB}^{(m)} = t_{A0,B0}(t_{A0,Bm} + t_{B0,Am})/U$. Then expression (2.1) can now be decomposed as $\mathbf{D}_{AB} = \mathbf{D}'_{AB} + \mathbf{D}''_{AB}$, with

$$\mathbf{D}'_{AB} = -2i \sum_{m \neq 0} \left(\frac{\lambda}{\Delta_m} \right) [\langle m_A|\mathbf{L}_A|0_A\rangle - \langle m_B|\mathbf{L}_B|0_B\rangle] J_{AB}^{(m)}, \tag{2.2}$$

$$\mathbf{D}''_{AB} = 2i \sum_{m \neq 0} \left(\frac{\lambda}{\Delta_m} \right) [\langle m_A|\mathbf{L}_A|0_A\rangle + \langle m_B|\mathbf{L}_B|0_B\rangle] I_{AB}^{(m)}. \tag{2.3}$$

Since we expect that $\Delta_m^A \simeq \Delta_m^B = \Delta_m$ is fulfilled with a good accuracy, this approximation is used in Eqs. (2.2) and (2.3).

With this preliminaries we are now able to predict the spatial pattern of DM vector distribution along magnetic chains in the *AF* and *F* structural configurations of $Sr_2V_3O_9$. Let us denote *AB* as the line fragment connecting the centers of neighboring $[VO_6]_A$ and $[VO_6]_B$ octahedra and define an auxiliary local axis $\mathbf{b}'$, which is parallel to $\mathbf{b}$ and passes through the midpoint of AB. Then a rotation by π angle about $\mathbf{b}'$ interchange $[VO_6]_A$ and $[VO_6]_B$ octahedra, including the ionic positions of V_A and V_B, if the *AF* type of the V ion off-center displacement is realized. This means that $\mathbf{b}'$ is a twofold rotation axis for each V_A-V_B neighbors in the case of *AF* structural configuration, while this local symmetry operation is lost in *F* configuration. Further, in *AF* configuration the symmetry requires for the transfer integrals the property $t_{B0,Am} = t_{A0,Bm}$, leading to $I_{AB}^{(m)} = 0$ for all m, which means $\mathbf{D}''_{AB} = 0$ and, hence, $\mathbf{D}_{AB}$ is specified by Eq. (2.2). By noting that for a given m, two vectors $\langle m_A|\mathbf{L}_A|0_A\rangle$ and $\langle m_B|\mathbf{L}_B|0_B\rangle$ are transformed to each other by a π rotation about $\mathbf{b}' \| \mathbf{b}$, Eq. (2.2) shows that the vector $\mathbf{D}_{AB}$ is confined to the ac plane, which is in accordance with Moriya's symmetry rules.[10] Moreover, the alternating tilt of the VO_6 octahedra along a magnetic chain provides a staggered variation of DM vectors, $\mathbf{D}_{\ell,\ell+1} = (-1)^\ell \mathbf{D}^{(s)}$, where ℓ denotes the V sites along a magnetic chain.

In the low symmetry *F*-configuration, one expects $I_{AB}^{(m)} \neq 0$ and, therefore, $\mathbf{D}_{AB}$ acquires an additional component $\mathbf{D}''_{AB}$ $(\neq 0)$ specified by Eq.(2.3). By using similar arguments as above, we obtain, first, that $\mathbf{D}''_{AB} \| \mathbf{b}$ and, second, that $\mathbf{D}''_{AB}$ is a uniform (non-staggered) component along a magnetic chain. Thus, in the *F*-configuration we predict the following variation of the DM vector along a magnetic chain: $\mathbf{D}_{\ell,\ell+1} = (-1)^\ell \mathbf{D}^{(s)} + \mathbf{D}^{(u)}$, with the staggered component $\mathbf{D}^{(s)}$ being confined to the ac-plane and the uniform component $\mathbf{D}^{(u)} \| \mathbf{b}$.

An equivalent description of the AFM spin-1/2 chain system, Eq. (1.1), with staggered DM vector, $\mathbf{D}_{\ell,\ell+1} = (-1)^\ell \mathbf{D}^{(s)}$, is based on the use of a nonuniform unitary transformation (rotation $\hat{R}_\ell$) in the spin space, $\mathbf{S}'_\ell = \hat{R}_\ell \mathbf{S}_\ell$. Alternating rotation by angle $\varphi_\ell = (-1)^\ell \arctan(D^{(s)}/2J)$ about $\mathbf{d}$ axis ($\mathbf{d} = \mathbf{D}^{(s)}/D^{(s)}$) eliminates the staggered DM interaction and leads to a renormalized isotropic exchange $J \to \overline{J} = J[1 + (D^{(s)})^2/2J^2]$ and a reduced symmetric anisotropy $\Gamma^{\alpha\beta} \to \overline{\Gamma}^{\alpha\beta} = \Gamma^{\alpha\beta} - [(D^{(s)})^2/2J] d^\alpha d^\beta$. With this result, the authors of Ref. 6 claim that the DM term contribution to the ESR linewidth is of the same level as that of symmetric anisotropy. If one neglects in Eq. (1.1) the original symmetric anisotropy, $\Gamma^{\alpha\beta} = 0$, then $\overline{\Gamma} \sim (D^{(s)})^2/J$ and the resulting ESR linewidth $\overline{\eta}$ in the high-T low-field limit is estimated to be $\overline{\eta} \sim \overline{\Gamma}^2/J \sim (D^{(s)})^4/J^3$, as discussed in Ref. 7. Assuming the standard estimate $D^{(s)} \sim (\Delta g/g)J$, one obtains also $\overline{\eta} \sim (\Delta g/g)^4 J$. Below we argue, however, that in the AFM chain system with staggered DM interaction the residual symmetric anisotropy and the expected resulting ESR linewidth are much smaller than the value $\overline{\eta}$ predicted in Ref. 7.

Actually, model (1.1) is the 1D realization of the general spin-1/2 Hamiltonian derived by Moriya[10] in the effective second-order perturbation calculation of the SE theory. Then, as argued in Ref. 12, if the DM vector is staggered, Hamiltonian (1.1) possesses a hidden symmetry. This means, after applying the nonuniform rotation in spin space, an exact cancellation, $\overline{\Gamma}^{\alpha\beta} = 0$, i.e., the residual anisotropic exchange disappear in the Moriya's second-order perturbation SE theory. A finite residual anisotropic exchange $\delta\Gamma$ is obtained if one includes higher-order corrections.[10] Close inspection allows us to predict the order of magnitude of $\delta\Gamma$ as

$$\delta\Gamma \sim \left(\frac{\Delta g}{g} \right)^2 J \left(\frac{J_H}{U} \right), \tag{2.4}$$

where J_H is the Hund's coupling constant of a magnetic ion under consideration. Therefore, in the high-T limit the residual ESR linewidth is expected to be

$$\eta_{res} \sim \left(\frac{\Delta g}{g} \right)^4 J \left(\frac{J_H}{U} \right)^2. \tag{2.5}$$

In a typical situation, J_H/U is in the range 0.1–0.3, so that the corresponding linewidth η_{res} is at least by an order of magnitude smaller than the value, $\overline{\eta} \sim (\Delta g/g)^4 J$, suggested in Ref. 7. In an applied magnetic field $\mathbf{H}$, the width η_{res} has to be compared with that coming from the transverse staggered field,[7] $h \sim DH/J$, to decide which contribution dominates the ESR linewidth in the high-T regime, $T \gg J$.

It is worth to specially emphasize that a strongly reduced ESR linewidth (2.5) is a manifestation of a hidden symmetry of the underlying model (1.1) with a *staggered* DM vector distribution. This symmetry disappears in the AFM chain system with a more general DM vector distribution. The standard Kubo and Tomita approach[13] predicts a more stronger line broadening with a width of $\eta_{DM} \sim D^2/J \sim (\Delta g/g)^2 J$.

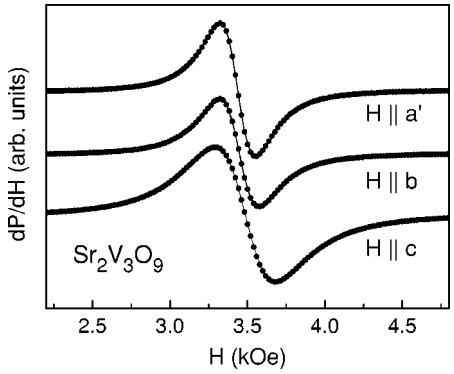

FIG. 2. ESR spectra (dP/dH, P: absorbed power) with the external magnetic field H applied along three different crystallographic directions a',b,c at $T=120$ K. The solid lines fit the spectra with Lorentzian lines.

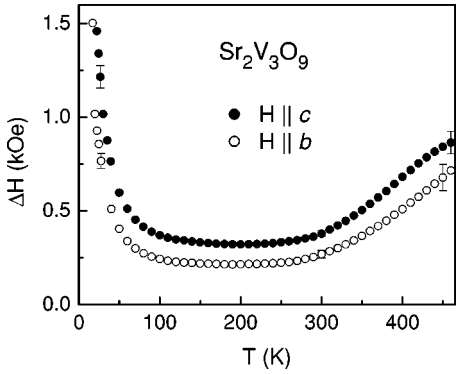

FIG. 3. Temperature dependence of the ESR linewidth ΔH measured for the magnetic field applied parallel to the crystallographic b and c axes.

III. EXPERIMENTAL PROCEDURE AND RESULTS

$Sr_2V_3O_9$ single crystals were obtained by a Traveling Solidification Zone method in which the melt (in a stationary crucible) was subjected to a strong vertical gradient of temperature. The crystal growth was performed in a vertical tube furnace, using platinum crucibles and a static Argon 6.0 atmosphere. The starting composition of the melt was not stoichiometric. It was composed by a mixture of pure $Sr_2V_3O_9$, VO_2, and V_2O_5. This was necessary because our differential thermal analysis (DTA) measurements showed that pure $Sr_2V_3O_9$ does not melt congruently but decomposes peritectically into $Sr_2V_2O_7$ plus liquid. Thus, the first compound to solidify is $Sr_2V_2O_7$. Adding a mixture of VO_2 and V_2O_5 inhibits the formation of $Sr_2V_2O_7$ and reduces the liquidus temperature. The $Sr_2V_3O_9$ crystals (with typical sizes of about $5\times4\times2$ mm^3) were easily cut from the batch. Their orientation and single crystallinity was determined by the Laue method and polarized light.

The ESR measurements were performed with a Bruker Elexsys E500 spectrometer at X-band frequencies (9.4 GHz). The temperature was controlled between 4 K and 500 K by continuous flow cryostats using helium gas or nitrogen gas. The samples were placed into quartz tubes and fixed with either paraffin (at low temperatures 4 K$\leqslant T\leqslant$300 K) or NaCl (at 300 K$\leqslant T\leqslant$500 K). A single ESR absorption line has been observed within the whole paramagnetic region and can be ascribed to V^{4+} ions. Figure 2 presents representative ESR spectra and their anisotropic behavior for three different crystallographic directions. Within the whole temperature range the spectra are well fitted with a Lorentzian line shape (solid lines in Fig. 2).

The observed ESR g factor (determined by the resonance field) is temperature independent. Along the crystallographic axes (a,a',b,c) the values are $g_a=1.957\pm0.001$, $g_{a'}=1.952\pm0.001$, $g_b=1.948\pm0.001$, and $g_c=1.931\pm0.001$. The deviation Δg from the free electron value g is rather small, $\Delta g/g\simeq0.03$, which is typical for vanadates bearing a weak spin-orbit coupling. The observed g factors result from an averaging of the individual g tensors of two inequivalent VO_6 octahedra that alternate along a magnetic chain. Because of this alternation, the individual g tensors acquire also a staggered component $g^{(s)}$, like in Cu-compounds with an alternating g tensor.[3–5] The resulting anisotropic Zeeman interaction contributes to the ESR linewidth broadening. A detailed analysis shows, however, that in $Sr_2V_3O_9$ the weak g-tensor anisotropy and the small tilt angle of VO_6 octahedra lead to a small staggered component, $g^{(s)}\approx0.01$, and the corresponding contribution to the ESR linewidth is $\approx1\%$ of the observed width. Therefore, we neglect this contribution in our further analysis.

The experimental ESR linewidth ΔH results as a fit parameter of a Lorentzian line shape and is measured as the half width at half maximum of the nonderived ESR line. ΔH is related to the notation η used in Sec. II as $\eta=g\mu_B\Delta H$, where g and μ_B are the average g factor and the Bohr magneton, respectively. The temperature dependence of the ESR linewidth $\Delta H_{b,c}$ is shown in Fig. 3 for two different orientations of the external magnetic field applied either along the crystallographic b axis or along the c axis. The almost parallel temperature characteristics of $\Delta H_{b,c}$ demonstrate a predominantly temperature-independent anisotropy of ΔH.

A drastic ESR line broadening below 100 K can be attributed to the rapid development of the intrachain spin correlations with a subsequent growth of critical 3D correlations due to the vicinity of Néel's temperature. When the temperature is lowered towards the critical temperature $T_{crit}=T_N=5$ K a power law $\Delta H_{crit}\propto(T-T_{crit})^{-\alpha}$ approximately describes the linewidth with $\alpha=1$. This value reflects the low-dimensional character of the ESR line when it is compared with the critical behavior of ΔH of typical antiferromagnets in the one-dimensional case,[15] such as $CuCl_2\cdot2NC_5H_5$ ($\alpha=0.5$), or in the three-dimensional case,[16] such as GdB_6 ($\alpha=1.5$). Furthermore, it was shown in the experimental review by Taylor and Coles[14] that in low-dimensional spin systems an essential broadening of the ESR line can occur in a rather broad temperature range of about $1.5\,T_N<T<10\,T_N$. Again, very similar ESR behavior near T_N was observed in different low-dimensional antiferromagnets such as $CuCl_2\cdot2NC_5H_5$,[15] $CsNiCl_3$,[17] and $LiCuVO_4$.[18]

For temperatures above 100 K the ESR linewidth enters the paramagnetic region where the spin-spin relaxation reaches an asymptotic value $\Delta H(J/kT\rightarrow0)$. Spin-lattice relaxation processes become dominant at temperatures above

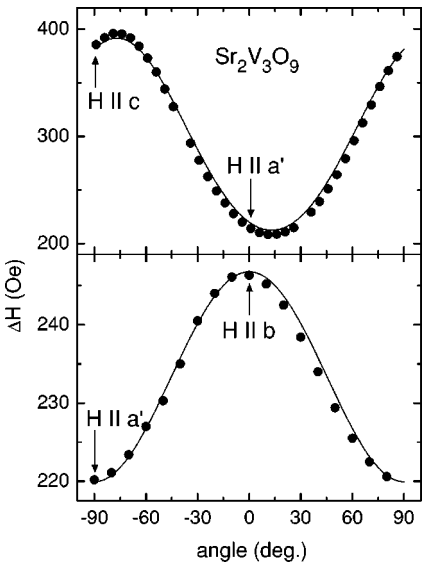

FIG. 4. The angular dependencies of the linewidth ΔH in $Sr_2V_3O_9$ observed in the $a'c$ and $a'b$ plane at $T=120$ K. The solid lines represent a fit according to Eqs. (4.1) and (4.3) with the parameters $D=3.08$, $d_x=0.23$, $d_y=0.41$, $d_z=0.89$.

270 K. Both the exact mechanism of the relaxation above 270 K and the type of critical broadening below 100 K are beyond the scope of the present paper. We treat the data in the range 100 K$<T<$270 K as the asymptotic high-T values and concentrate the further discussion solely on the data obtained at $T=120$ K as representative values.

The angular dependencies of the ESR linewidth ΔH observed when rotating the external field H in the $a'c$ and $a'b$ planes are shown in Fig. 4 together with theoretical fittings according to Sec. IV. We recall that the auxiliary a' axis lying in the ac plane is perpendicular to the b and c axes. Within the $a'c$ plane a stronger anisotropy of ΔH is seen and a particular direction close to the c axis is indicated by a maximum of the linewidth.

IV. LINEWIDTH ANALYSIS

The linewidth ΔH of a Lorentzian-shaped ESR absorption is determined by the second moment $M_2(J/kT)$ of the local magnetic fields due to anisotropic interactions as[13]

$$\Delta H=\frac{M_2(J/kT)}{g\mu_B\hbar\omega_{ex}}, \tag{4.1}$$

where $\omega_{ex}\approx J/\hbar$ is the exchange frequency. In the asymptotic regime the temperature independent second moment $M_2(J/kT\rightarrow 0)$ can be expressed via the microscopic spin-Hamiltonian parameters and a particular angular dependence of $M_2(J/kT\rightarrow 0)$ is caused mainly by the form of the dominant anisotropy. In the case of $Sr_2V_3O_9$, by taking simple estimations for different contributions to the second moment (as the squares of corresponding spin-Hamiltonian parameters), one can easily see that the contributions due to hyperfine and magnetic dipole-dipole interactions are negligible, like that of the anisotropic Zeeman interaction discussed before. The interchain anisotropic interactions are also expected to be of minor importance and the main source to the ESR line broadening is due to intrachain exchange anisotropies.

To size up the antisymmetric DM interaction $\sim D$ and the symmetric anisotropy $\sim\Gamma$, approximate relations $D\approx(\Delta g/g)J\Phi$ and $\Gamma\approx(\Delta g/g)^2J$ are usually used. If the DM interaction is not suppressed by a small geometrical factor Φ, then for $\Phi\sim 1$ and $\Delta g/g\ll 1$ the antisymmetric anisotropy dominates and provides the main contribution $g\mu_B\Delta H_{DM}\sim D^2/J\sim(\Delta g/g)^2J$ to the line broadening. The above expression for ΔH_{DM} is obtained by the direct application of the Kubo-Tomita formula (4.1) to the DM interaction without specifying a space distribution of the DM vector. With the values $\Delta g/g\simeq 0.03$ and $J\simeq 82$ K characteristic to $Sr_2V_3O_9$, one obtains $\Delta H_{DM}\sim 500$ Oe, the order of which approximately agrees with the observation. At the same time, the contribution due to the symmetric exchange anisotropy is smaller by the factor $(\Delta g/g)^2\approx 10^{-3}$. As pointed out in Refs. 6,7 and discussed in Sec. II, in the case of a staggered DM interaction, a hidden symmetry in the chain system strongly reduces the anisotropy of spin-spin interaction and, hence, one expects a significantly narrowed resonance line. In this case, a direct application of the Kubo-Tomita formula to the DM interaction is incorrect and we estimate the linewidth relying on Eq. (2.5). Then, the expected residual linewidth in $Sr_2V_3O_9$ becomes of the order $\Delta H_{res}\sim 1$ Oe, which is much smaller than the observed $\Delta H\sim 300$ Oe. Note that, in the actual case of a low applied field ~ 3 kOe, the staggered field contribution[7] to the linewidth is negligible. These results clearly show that in $Sr_2V_3O_9$ the chain model with a staggered DM interaction is not applicable. The alternative model, advanced in Sec. II and corresponding to the F configuration of the V-ion displacements, suggests the following form of the DM vector variation along a chain:

$$\mathbf{D}_{\ell,\ell+1}=(-1)^{\ell}\mathbf{D}^{(s)}+\mathbf{D}^{(u)}. \tag{4.2}$$

Here the staggered component $\mathbf{D}^{(s)}$ is confined to the ac plane and the uniform component $\mathbf{D}^{(u)}$ is parallel to the b axis. Below, using this model, the angular dependence of the ESR linewidth ΔH_{DM} is determined from Eq. (4.1) and compared with the observation.

Note, first, that according to (4.2) there are two inequivalent DM vectors, $\mathbf{D}_1=\mathbf{D}_{\ell-1,\ell}$ and $\mathbf{D}_2=\mathbf{D}_{\ell,\ell+1}$, which alternate each other along a magnetic chain. These two vectors are transformed to each other by π rotation about the **b** axis. Introducing a (x,y,z) coordinate system, which is attached to the $(\hat{\mathbf{a}}',\hat{\mathbf{b}},\hat{\mathbf{c}})$ basis, the vectors $\mathbf{D}_1$ and $\mathbf{D}_2$ can be written as follows: $\mathbf{D}_1=D(d_x,d_y,d_z)$ and $\mathbf{D}_2=D(-d_x,d_y,-d_z)$, where $d_\alpha(\alpha=x,y,z)$ are Cartesian components of a unit vector **d**. The effect of the DM interaction on the second moment in (4.1) is calculated by using a standard derivation procedure.[18,19] This yields

$$M_2^{DM}=\tfrac{1}{4}D^2[d_x^2(1+\sin^2\theta\cos^2\varphi)+d_y^2(1+\sin^2\theta\sin^2\varphi)+d_z^2(1+\cos^2\theta)+d_xd_z\sin 2\theta\cos\varphi]. \tag{4.3}$$

Here the polar angle θ and the azimuth angle φ of the applied magnetic field are measured with respect to the c and a'

axes. To describe the experimental results of ΔH in the asymptotic regime with Eqs. (4.1) and (4.3), only three parameters should be adjusted. Namely, these are the strength of DM interaction D and two components of the unit vector **d**. The result of a fit to the angular dependence of the linewidth at 120 K in both the $a'c$ and the $a'b$ planes is shown in Fig. 4. We note, first, that the resulting strength $D=3.08$ K is close to the expected value obtained by the standard theoretical estimate $D\sim(\Delta g/g)J\approx 2.5$ K and, second, the theoretical curves with the directional parameters $d_x=0.23, d_y=0.41, d_z=0.89$ reproduce strikingly well the experimentally observed anisotropy of ΔH. Most obviously the maximum of ΔH in the $a'c$ plane appears at an angle of 75.5°, which is nicely reproduced by the experimental data (see Fig. 4, upper frame). Therefore, the intralayer F configuration, where the V-ion off-center displacements of two neighboring structural chains are in phase, is favorable to explain the ESR results on $Sr_2V_3O_9$.

V. CONCLUSION

In summary, we performed a study of the angular and temperature dependence of the electron spin resonance in the quasi-one-dimensional spin-1/2 antiferromagnetic vanadate $Sr_2V_3O_9$. The antisymmetric Dzyaloshinskii-Moriya exchange anisotropy within V chains was shown to dominate strongly the other anisotropies and was successfully applied to describe both size and orientation dependence of the ESR linewidth ΔH in the high-temperature limit. As a necessary background, we developed a theoretical analysis to relate the peculiarities of the V-chain lattice structure in $Sr_2V_3O_9$ with the spatial pattern of the Dzyaloshinskii-Moriya vector distribution along a chain. Two different spatial patterns are considered for the theoretical description of ΔH. In the case of a staggered Dzyaloshinskii-Moriya interaction, improvements of a recently developed ESR theory based on a hidden symmetry are suggested. Both the improved theory and the standard one are applied to distinguish between the two patterns of the Dzyaloshinskii-Moriya vector intrachain distributions. Comparison with experimental results clearly indicated the presence of the nonstaggered distribution of the DM vector in $Sr_2V_3O_9$. Such an exchange anisotropy makes the understanding of the magnetic properties of this chainlike system a challenging problem.

ACKNOWLEDGMENTS

We acknowledge valuable discussions with H.-A. Krug von Nidda, M.V. Eremin, V.E. Kataev, and A.I. Smirnov. V.A. Ivanshin was supported in part by the Swiss National Science Foundation (Grant No. 7SUPJ062258). D. V. Zakharov was supported by the CRDF grant (Grant No. REC-007).

[1] P.Y. Zavalij and M.S. Whittingham, Acta Crystallogr., Sect. B: Struct. Sci. **55**, 627 (1999).
[2] E.E. Kaul, H. Rosner, V. Yushankhai, J. Sichelschmidt, R.V. Shpanchenko, and C. Geibel, Phys. Rev. B **67**, 174417 (2003).
[3] R. Feyerherm, S. Abens, D. Günther, T. Ishida, M. Meißner, M. Meschke, T. Nogami, and M. Steiner, J. Phys.: Condens. Matter **12**, 8495 (2000).
[4] D.C. Dender, D. Davidovic, D.H. Reich, C. Broholm, K. Lefmann, and G. Aeppli, Phys. Rev. B **53**, 2583 (1996).
[5] I. Affleck and M. Oshikawa, Phys. Rev. B **60**, 1038 (1999).
[6] J. Choukroun, J.-L. Richard, and A. Stepanov, Phys. Rev. Lett. **87**, 127207 (2001).
[7] M. Oshikawa and I. Affleck, Phys. Rev. B **65**, 134410 (2002).
[8] A. Abragam, and B. Bleaney, *Electron Paramagnetic Resonance of Transition Ions* (Dover, New York, 1970).
[9] B. Schmidt, V. Yushankhai, L. Siurakshina, and P. Thalmeier, Eur. Phys. J. B **32**, 43 (2003).
[10] T. Moriya, Phys. Rev. **120**, 91 (1960).
[11] F. Keffer, Phys. Rev. **126**, 896 (1962).
[12] T.A. Kaplan, Z. Phys. B: Condens. Matter **49**, 313 (1983); L. Shekhtman, O. Entin-Wohlman, and A. Aharony, Phys. Rev. Lett. **69**, 836 (1992).
[13] R. Kubo and K. Tomita, J. Phys. Soc. Jpn. **9**, 888 (1954).
[14] R.H. Taylor and B.R. Coles, J. Phys. F: Met. Phys. **5**, 121 (1974); **4**, 303 (1973).
[15] Y. Ajiro, S. Matsukawa, T. Yamada, and T. Haseda, J. Phys. Soc. Jpn. **39**, 259 (1975).
[16] G. Sperlich, K.H. Janneck, and K.H.J. Buschow, Phys. Status Solidi B **57**, 701 (1973).
[17] S.S. Sosin, I.A. Zaliznyak, L.A. Prozorova, Yu.M. Tsipenyuk, and S.V. Petrov, JETP **85**, 114 (1997).
[18] H.-A. Krug von Nidda, L.E. Svistov, M.V. Eremin, R.M. Eremina, A. Loidl, V. Kataev, A. Validov, A. Prokofiev, and W. Aßmus, Phys. Rev. B **65**, 134445 (2002).
[19] Z.G. Soos, K.T. McGregor, T.T.P. Cheung, and A.J. Silverstein, Phys. Rev. B **16**, 3036 (1977).